

CDF Results on B Decays

JOHN E. SKARHA*

Department of Physics and Astronomy
The Johns Hopkins University
Baltimore, Maryland 21218, USA

ABSTRACT

We present recent CDF results on B lifetimes, B meson mass measurements, ratios of branching ratios, and rare decays. In addition, we present the first measurement of time-dependent B_d mixing at CDF. Several results have been updated and a few new ones included since the workshop.

1. Introduction

During the 1992-95 Tevatron collider Run I, the Collider Detector at Fermilab (CDF)¹ has so far collected a data sample of $\bar{p}p$ collisions at $\sqrt{s} = 1.8$ TeV with an integrated luminosity of $> 95 \text{ pb}^{-1}$. This was split into two separate data-taking runs: Run 1a ($\sim 20 \text{ pb}^{-1}$) and the present Run 1b ($> 75 \text{ pb}^{-1}$). Data-taking is planned to continue through 1995 and a total sample of at least 120 pb^{-1} is expected. This data sample, in combination with improvements to the data acquisition system, the muon coverage, and most importantly, the installation of the CDF SVX silicon vertex detector,² has allowed many new results on B decays. In this paper we report results on B lifetimes, ratios of branching ratios, rare decays, and B meson mass measurements. In addition, we present the first CDF measurement of time-dependent B_d mixing.

2. B^+ and B^0 Meson Lifetimes

Increasingly precise measurements of the B^+ and B^0 lifetimes are important for testing the predicted B hadron lifetime hierarchy and to measure the relative contributions from non-spectator decays. Only small lifetime differences are expected between the B^+ and B^0 mesons ($\sim 5\%$ ³) and experiments are now approaching this precision.

At CDF, the measurement of the charged and neutral B meson lifetimes has been performed using fully reconstructed B decays in the following modes⁴:

$$\begin{array}{llll}
 B^+ & \rightarrow J/\psi K^+ & \rightarrow \mu^+ \mu^- K^+; & B^+ & \rightarrow J/\psi K^*(892)^+ & \rightarrow \mu^+ \mu^- K_S^0 \pi^+ \\
 B^+ & \rightarrow \psi(2S) K^+ & \rightarrow \mu^+ \mu^- \pi^+ \pi^- K^+; & B^+ & \rightarrow \psi(2S) K^*(892)^+ & \rightarrow \mu^+ \mu^- \pi^+ \pi^- K_S^0 \pi^+ \\
 B^0 & \rightarrow J/\psi K_S^0 & \rightarrow \mu^+ \mu^- K_S^0; & B^0 & \rightarrow J/\psi K^*(892)^0 & \rightarrow \mu^+ \mu^- K^+ \pi^- \\
 B^0 & \rightarrow \psi(2S) K_S^0 & \rightarrow \mu^+ \mu^- \pi^+ \pi^- K_S^0; & B^0 & \rightarrow \psi(2S) K^*(892)^0 & \rightarrow \mu^+ \mu^- \pi^+ \pi^- K^+ \pi^-
 \end{array}$$

*For the CDF Collaboration; Contribution to the proceedings of the LISHEP95 Workshop on Heavy Flavor Physics, Rio de Janeiro, Brazil, February 20-22, 1995.

The capability of using exclusive decay modes is unique to CDF, no other experiment has large samples of fully reconstructed B decays that can be used for lifetime measurements. B^+ and B^0 lifetime measurements using exclusive decays have been previously published for the $\sim 20 \text{ pb}^{-1}$ Run 1a data sample.⁵

CDF has recently added an additional $\sim 48 \text{ pb}^{-1}$ of $J/\psi \rightarrow \mu^+\mu^-$ data from Run 1b, bringing the total data sample to 67.7 pb^{-1} . As in the Run 1a analysis, reconstruction of $J/\psi \rightarrow \mu^+\mu^-$ candidates is the starting point. The $\psi(2S) \rightarrow J/\psi\pi^+\pi^-$ decays are then searched for in that data sample. Two track combinations are used to find the $K^*(892)^0$ and K_S^0 candidates. The $\psi(2S)$ and K_S^0 candidates are required to be within $20 \text{ MeV}/c^2$, while J/ψ and K^* candidates are required to be within $80 \text{ MeV}/c^2$ of their respective world average values.⁶ The invariant mass distributions of the J/ψ and $\psi(2S)$ are shown in Figure 1.

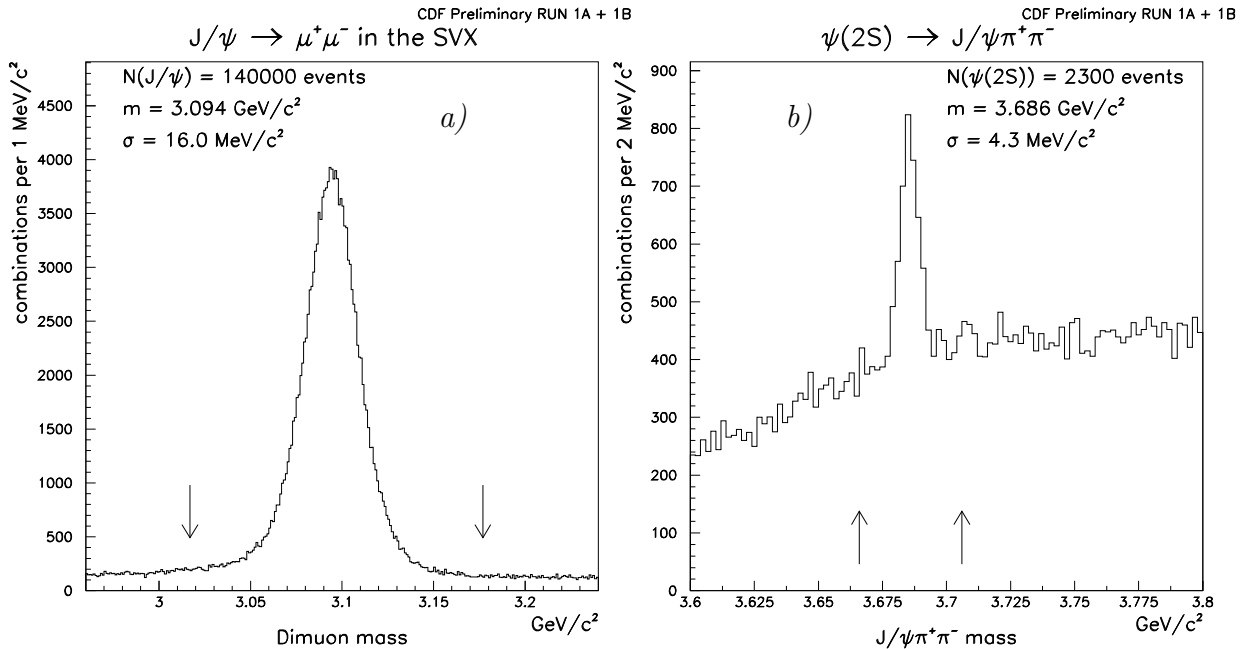


Figure 1: Mass distributions of the a) J/ψ and b) $\psi(2S)$. The mass cuts are indicated.

The K^+ , K_S^0 , and $K^*(892)$ candidates must have $p_T > 1.25 \text{ GeV}/c$ in order to be combined with a J/ψ or $\psi(2S)$ to reconstruct a B meson. Individual cuts of $p_T(K) > 1.0$ and $p_T(\pi) > 0.5 \text{ GeV}/c$ are also required for $K^*(892)^0$ candidates.

In the final B reconstruction, all the decay tracks, except those from a K_S^0 , are vertex constrained, and the J/ψ and $\psi(2S)$ candidates are mass constrained to their world average values. Any B mesons with $p_T < 6.0 \text{ GeV}/c$ are rejected. In the case of multiple candidates per event, only the one with the best χ^2 from the constrained fit is kept.

The upper plots in Figure 2 show the invariant mass distributions of all B^+ and B^0 candidates. Background in these distributions comes from combinations of J/ψ 's with tracks produced during the b -quark fragmentation or with other remnants of the

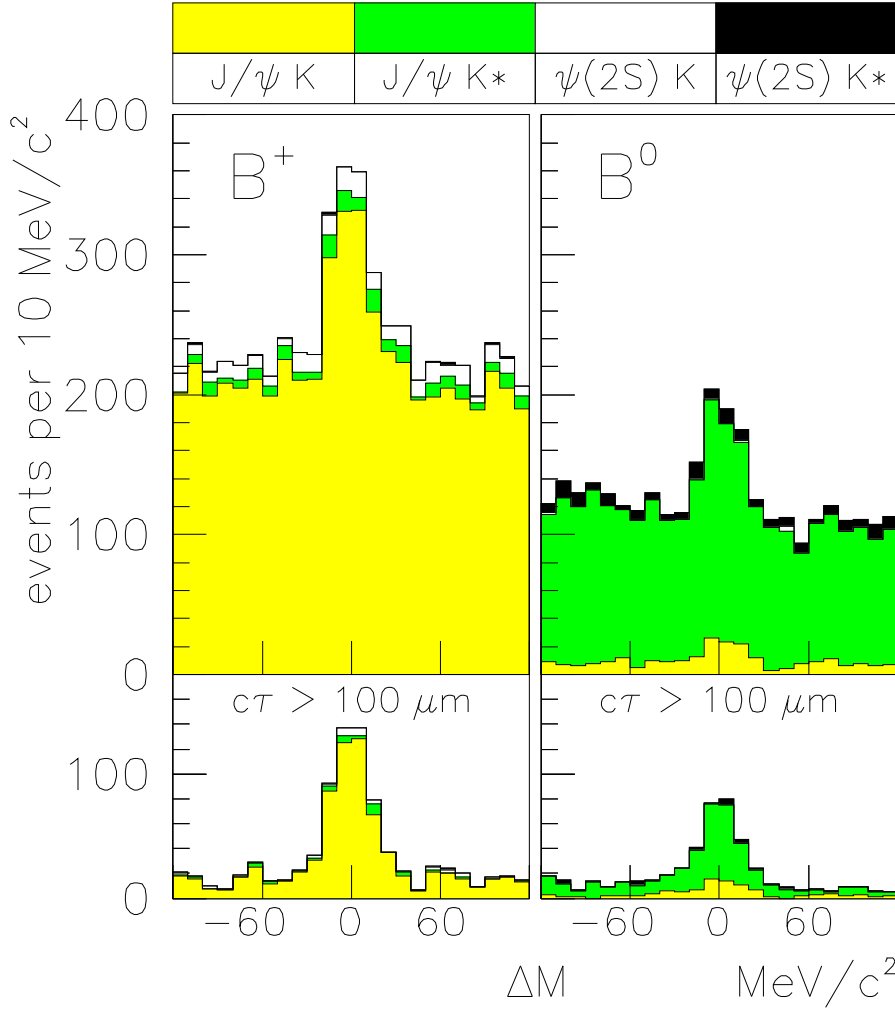


Figure 2: Mass distributions of the fully reconstructed B samples, both with (upper) and without (lower) a $c\tau > 100 \mu\text{m}$ cut. (CDF Preliminary)

$p\bar{p}$ collision. These tracks should reconstruct to the primary vertex and consequently the background is smallest for events where the decay distance is large. This is demonstrated in the lower plots of Figure 2 where a $c\tau > 100 \mu\text{m}$ cut is made to illustrate this point. The contributions from the different decay modes is given by the shading and, as expected, the $B^+ \rightarrow J/\psi K^+$ decay is dominant for charged B 's and the $B^0 \rightarrow J/\psi K^*(892)^0$ channel has the largest rate for neutral B 's.

For the lifetime analysis, we define the signal region to be within $\pm 30 \text{ MeV}/c^2$ of the world average B mass.⁶ Sideband regions are defined to be between 60 and 120 MeV/c^2 away from the world average. This selection excludes the mass region where B 's with a missing π would be typically reconstructed.

The B^+ and B^0 proper decay length distributions, for both the signal and sideband regions, are shown in Figure 3. The superimposed curves are the results of sepa-

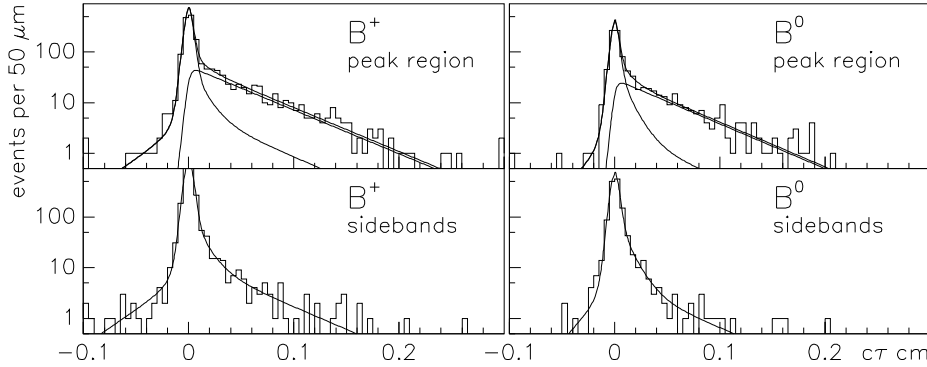


Figure 3: The proper decay length ($c\tau$) distributions of the fully reconstructed B samples. The fits (curves) are described in the text. (CDF Preliminary)

rate unbinned likelihood fits for the B^+ and B^0 lifetimes. The signal region fit consists of a lifetime exponential convoluted with a Gaussian resolution function, while the background is modeled with a Gaussian plus asymmetric exponential tails. The signal and background distributions are fit simultaneously. The fits indicate that there are 524 ± 29 charged and 285 ± 21 neutral B mesons in the signal regions. There is some residual positive lifetime component to the background due to resolution effects in which $B \rightarrow J/\psi K \pi^0$ decays are reconstructed in the B mass sideband region. The results of the lifetime fits to the $c\tau$ distributions are $c\tau^+ = 503 \pm 26 \mu\text{m}$ and $c\tau^0 = 492 \pm 34 \mu\text{m}$.

Residual misalignment, trigger bias, and beam stability give the dominant contributions to the systematic uncertainty. However, these are common to the B^+ and B^0 lifetime measurements and cancel in the lifetime ratio. The other systematic contributions are significantly reduced compared to the previous Run 1a analysis due to the increased stability of the $c\tau$ distributions from the larger statistics. Table 1 gives the sources of systematic uncertainty.

In the combined Run 1a + 1b data sample (67.7 pb^{-1}), the preliminary measurements of τ^+ , τ^0 , and τ^+/τ^0 using exclusive $B \rightarrow J/\psi K$ decays are:

$$\begin{aligned} \tau_{excl}^+ &= 1.68 \pm 0.09 \text{ (stat)} \pm 0.06 \text{ (syst)} \text{ ps} \\ \tau_{excl}^0 &= 1.64 \pm 0.11 \text{ (stat)} \pm 0.06 \text{ (syst)} \text{ ps} \\ (\tau^+/\tau^0)_{excl} &= 1.02 \pm 0.09 \text{ (stat)} \pm 0.01 \text{ (syst)} \end{aligned}$$

We see that the uncertainty on the B^+ (B^0) lifetime is only 6.4% (7.6%) and the precision on the lifetime ratio is dominated by statistics and is less than 10%.

We now turn to a measurement of the charged and neutral B meson lifetimes using semileptonic decays, as has been previously done by several LEP experiments.⁷ Partially reconstructed semileptonic decays of B mesons, namely a lepton in association with a D^0 or D^{*+} meson will provide *nearly orthogonal* samples of charged and neutral B mesons and thus enable a determination of their individual lifetimes.

This new preliminary measurement uses both the single electron and muon samples in the $\sim 20 \text{ pb}^{-1}$ Run 1a data. Four sources of D^0 mesons are considered in this

Source of Uncertainty	B^+	B^0
Residual misalignment	10 μm	10 μm
Trigger bias	11 μm	11 μm
Beam stability	8 μm	8 μm
Resolution (scale)	1 μm	1 μm
Resolution (tails)	1 μm	4 μm
Background shape	1 μm	2 μm
Fitting procedure bias	2 μm	1 μm
Total	17 μm	18 μm

Table 1. Summary of systematic uncertainties for the exclusive B^+ and B^0 lifetime measurements.

analysis: 1) $B^- \rightarrow l^- \bar{\nu} D^0 X$, $D^0 \rightarrow K^- \pi^+$, where the D^0 is *not* from $D^{*+} \rightarrow D^0 \pi_s^+$ (“ D^0 sample”); 2) $\bar{B}^0 \rightarrow l^- \bar{\nu} D^{*+} X$, $D^{*+} \rightarrow D^0 \pi_s^+$, $D^0 \rightarrow K^- \pi^+$ (“ $D^{*+}, D^0 \rightarrow K^- \pi^+$ sample”); 3) $\bar{B}^0 \rightarrow l^- \bar{\nu} D^{*+} X$, $D^{*+} \rightarrow D^0 \pi_s^+$, $D^0 \rightarrow K^- \pi^+ X$ (“satellite sample”); and 4) $\bar{B}^0 \rightarrow l^- \bar{\nu} D^{*+} X$, $D^{*+} \rightarrow D^0 \pi_s^+$, $D^0 \rightarrow K^- \pi^+ \pi^+ \pi^-$ (“ $D^{*+}, D^0 \rightarrow K^- \pi^+ \pi^+ \pi^-$ sample”). The decay length of the D^0 projected onto the lepton-charm momentum in the plane transverse to the colliding beams, L_{XY} , must satisfy $L_{XY} > 0$ for the D^0 and satellite samples. Figure 4a shows the resulting $K^- \pi^+$ mass distribution, containing 560 ± 40 events in the D^0 peak, for the D^0 sample. Figure 4b gives the mass difference distribution for the $D^{*+}, D^0 \rightarrow K^- \pi^+$ sample, while Figures 5a and 5b give the Δm distributions for the satellite sample and $D^{*+}, D^0 \rightarrow K^- \pi^+ \pi^+ \pi^-$ samples, respectively. These figures show the production of $l^- D^0$ combinations in the expected (“right sign”) charge combinations and little evidence of any signal above combinatoric background in the “wrong sign” combinations.

The lepton and D^0 tracks are intersected to determine the B decay vertex position and decay length from the primary vertex. Since the B is only partially reconstructed, the $l^- D^0$ system transverse momentum can be used to determine a “pseudo- $c\tau$ ” value $c\tau^* = L_B m_B / p_T(l + D^0) = c\tau / K$, where K is a momentum correction factor determined from Monte Carlo. It is determined separately for each D^0 signal sample.

The signal $c\tau^*$ distributions are fit with an exponential lifetime term convoluted with a Gaussian resolution function and the momentum correction distribution. The lifetime of the background in the signal region is determined from the wrong sign and signal sideband distributions and is modeled by a Gaussian resolution function plus exponential tails. Figure 6 shows the results of the lifetime fits in the D^0 and satellite signal samples. The fit quality and results for the other D^{*+} samples are similar. The fraction of B^- and \bar{B}^0 contributing to each of the D^0 , D^{*+} , and satellite samples is determined and includes the effects of cross-talk due to: 1) the π_s^+ reconstruction efficiency, $\epsilon(\pi_s^+) = 0.93^{+0.07}_{-0.21}$. A missed spectator pion from D^{*+} decay can cause a D^0 to be associated with B^- rather than \bar{B}^0 ; 2) the D^{**} fraction, $f^{**} = \text{BR}(\bar{B} \rightarrow$

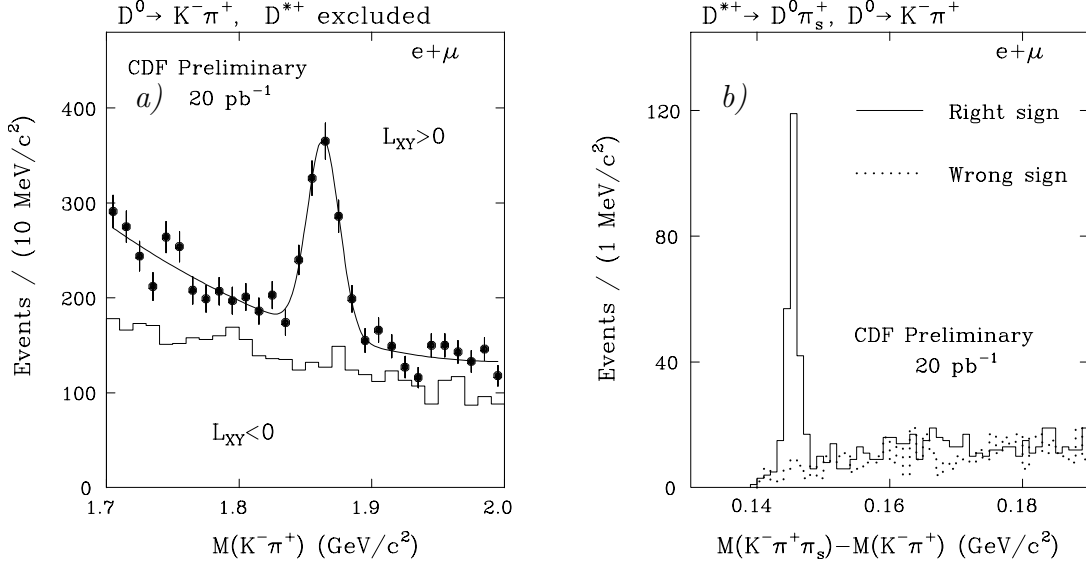


Figure 4: a) The $K^-\pi^+$ invariant mass distribution. Events from D^{*+} decay are excluded.

b) The distribution of the mass difference, $\Delta m = m(K^-\pi^+\pi_s) - m(K^-\pi^+)$, for $D^{*+} \rightarrow D^0\pi_s^+$, $D^0 \rightarrow K^-\pi^+$ candidates.

$l^-\bar{\nu}D^{**})/\text{BR}(\bar{B} \rightarrow l^-\bar{\nu}X) = 0.36 \pm 0.12$; 3) the fraction of D^{**} decaying to D^* , from Monte Carlo simulation is found to be $\text{BR}(D^{**} \rightarrow D^*\pi)/(\text{BR}(D^{**} \rightarrow D^*\pi) + \text{BR}(D^{**} \rightarrow D\pi)) = 0.78$; and 4) the charged-to-neutral lifetime ratio can affect the event mixture, $\text{BR}(B^- \rightarrow l^-\bar{\nu}X)/\text{BR}(\bar{B}^0 \rightarrow l^-\bar{\nu}X) = \tau(B^-)/\tau(\bar{B}^0)$. In spite of these effects, we find that the D^0 and D^{*+} signals provide *nearly orthogonal* samples of B^- and \bar{B}^0 mesons. A combined likelihood function is used to simultaneously fit the signal samples for the B^- and \bar{B}^0 meson lifetimes. Variations in the sample composition due to the above effects are included in the systematic uncertainty. The results are:

$$\begin{aligned} \tau_{semi}^+ &= 1.51 \pm 0.12 \text{ (stat)} \pm 0.08 \text{ (syst)} \text{ ps} \\ \tau_{semi}^0 &= 1.57 \pm 0.08 \text{ (stat)} \pm 0.07 \text{ (syst)} \text{ ps} \\ (\tau^+/\tau^0)_{semi} &= 0.96 \pm 0.10 \text{ (stat)} \pm 0.05 \text{ (syst)} \end{aligned}$$

We can separate out the relatively small correlations between the exclusive and semileptonic mode lifetime measurements due to residual misalignment and beam stability and compute CDF average values for τ^+ , τ^0 , and τ^+/τ^0 . We find:

$$\begin{aligned} \tau_{CDF}^+ &= 1.62 \pm 0.09 \text{ ps} \\ \tau_{CDF}^0 &= 1.60 \pm 0.09 \text{ ps} \\ (\tau^+/\tau^0)_{CDF} &= 1.00 \pm 0.07 \end{aligned}$$

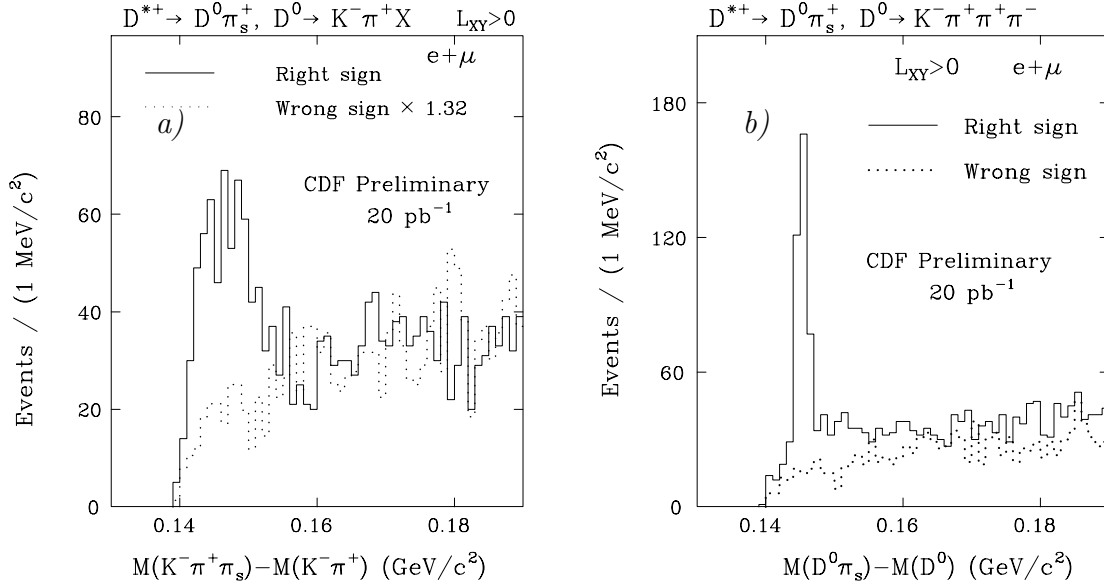


Figure 5: The mass difference distribution for a) $D^{*+} \rightarrow D^0 \pi_s^+, D^0 \rightarrow K^- \pi^+ X$ (satellite) and b) $D^{*+} \rightarrow D^0 \pi_s^+, D^0 \rightarrow K^- \pi^+ \pi^+ \pi^-$ candidates.

These can be compared to the latest LEP B lifetime averages⁹:

$$\begin{aligned}\tau_{LEP}^+ &= 1.68 \pm 0.07 \text{ ps} \\ \tau_{LEP}^0 &= 1.56 \pm 0.07 \text{ ps} \\ (\tau^+/\tau^0)_{LEP} &= 1.08 \pm 0.08\end{aligned}$$

These results are in good agreement and the precision on the CDF lifetime averages is now nearly identical to the latest LEP values.

3. B_s Meson Lifetime

A similar technique has been used to measure the B_s meson lifetime using semileptonic $B_s \rightarrow l \bar{\nu} D_s, D_s \rightarrow \phi \pi, \phi \rightarrow K^+ K^-$ decays.¹⁰ Precision measurement of the B_s meson lifetime is particularly important since it has been suggested by recent theory calculations that the lifetime between the two CP eigenstates produced by the mixing of the B_s and \bar{B}_s may be different by as much as 20%.¹¹ Such an effect should manifest itself as a difference in lifetimes between the B_s semileptonic decay, which is an equal mixture of the two CP states, and the decay $B_s \rightarrow J/\psi \phi$, which is expected to be dominated by the CP even state. Figure 7a shows the $K^+ K^- \pi^+$ invariant mass spectrum after all cuts for the combined electron and muon samples. Some 76 ± 8 events are found in the right-sign mass peak and a hint of the Cabbibo suppressed $D^+ \rightarrow \phi \pi^+$ decay is seen. Following the same procedure as above, the B_s lifetime from semileptonic $B_s \rightarrow l \bar{\nu} D_s$ is measured to be (Figure 7b):

$$\tau_s^{semi} = 1.42_{-0.23}^{+0.27} \text{ (stat)} \pm 0.11 \text{ (syst)} \text{ ps}$$

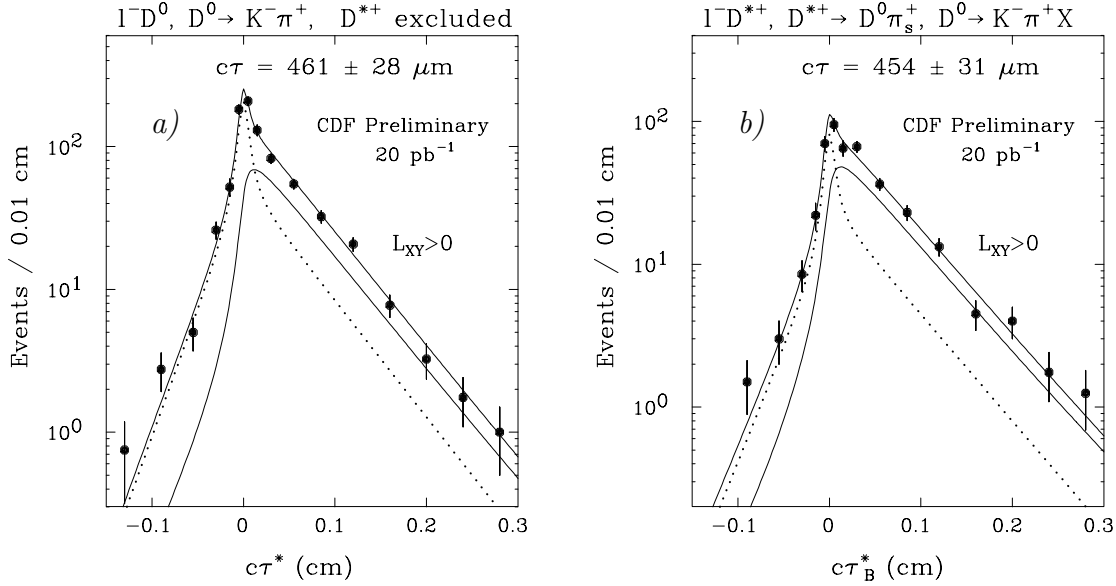


Figure 6: Distribution of pseudo- $c\tau$ for the a) D^0 and b) satellite samples.

Finally, there is a new low-statistics measurement of the B_s lifetime using fully reconstructed $B_s \rightarrow J/\psi\phi$, $J/\psi \rightarrow \mu^+\mu^-$, $\phi \rightarrow K^+K^-$ decays.¹⁰ At least two of the four daughter tracks are required to be reconstructed in the SVX. Based on a sample of 10 events, the B_s lifetime using exclusive $B_s \rightarrow J/\psi\phi$ is measured to be:

$$\tau_s^{excl} = 1.74_{-0.69}^{+1.08} \text{ (stat)} \pm 0.07 \text{ (syst)} \text{ ps}$$

Both of these measurements will greatly benefit from the addition of the Run 1b data and a first measurement of the $B_{s,long} - B_{s,short}$ lifetime difference should be possible.

4. B Meson Mass Measurements

The CDF B^+ , B^0 , and B_s mass measurements in the Run 1a data were reported previously.¹² The work continues to evaluate the tracking systematics in the current Run 1b data. Sizeable samples of fully reconstructed $B^+ \rightarrow J/\psi K^+$, $B^0 \rightarrow J/\psi K^*(892)^0$, $B^0 \rightarrow J/\psi K_S^0$, and $B_s \rightarrow J/\psi\phi$ decays will be available for precision B mass measurements in the combined Run 1a + 1b data sample. Figures 8a, 8b, and 9a give the reconstructed mass peaks currently under analysis after standard selection cuts.

5. Ratio of Branching Ratios

Using its large sample of $J/\psi \rightarrow \mu^+\mu^-$ decays, CDF has measured the ratio of branching ratios for many exclusive B decay modes involving a J/ψ in the final state. Table 2 lists the latest preliminary measurements. Of particular interest

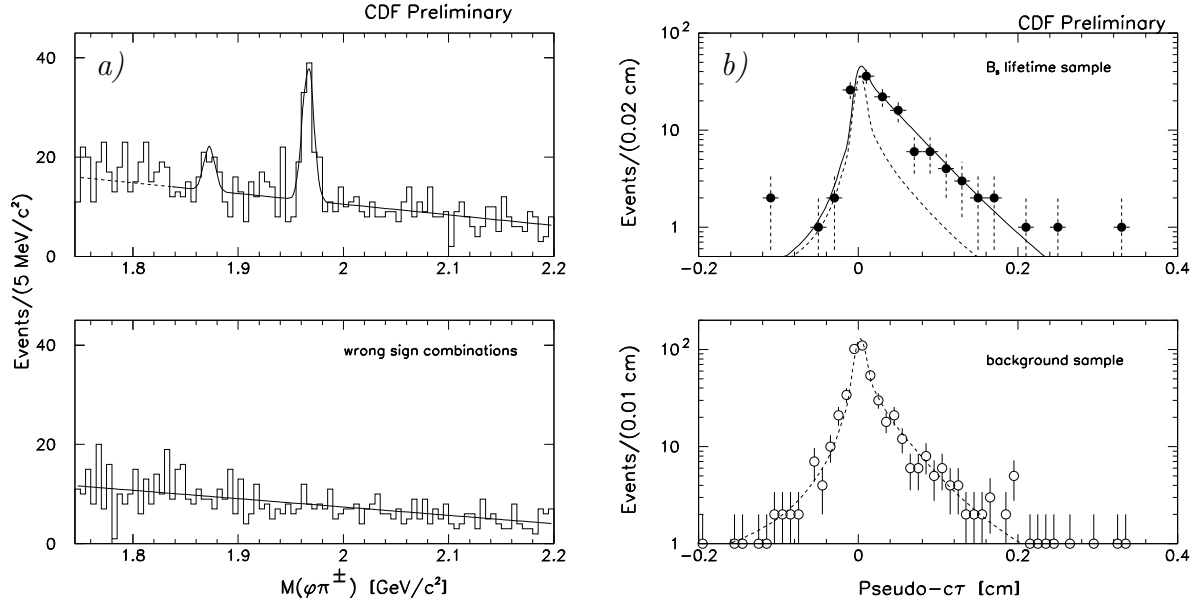


Figure 7: a) The $\phi\pi^-$ mass distribution for “right sign” and “wrong sign” lepton- D_s combinations. b) Pseudo- $c\tau$ distribution of the $l^-D_s^+$ signal sample showing the lifetime fits of the combined (signal plus background) and background distributions separately.

is the updated $BR(B_d \rightarrow J/\psi K^0)/BR(B_u \rightarrow J/\psi K^+)$ result and a new observation of Cabbibo-suppressed $B^+ \rightarrow J/\psi\pi^+$ decays (Figure 9b) and a measurement of $BR(B_u \rightarrow J/\psi\pi^+)/BR(B_u \rightarrow J/\psi K^+)$. This latter result is in good agreement with theoretical expectations and the recent CLEO measurement of $(4.3 \pm 2.3)\%$.¹³

The $b \rightarrow$ hadron fractions and their errors remain to be determined at the Tevatron. However, if we assume that $\frac{f(b \rightarrow B_d)}{f(b \rightarrow B_u)} = \frac{0.375}{0.375} = 1.0$ and $\frac{f(b \rightarrow B_s)}{f(b \rightarrow B_d)} = \frac{0.15}{0.375} = 0.40$, then we obtain the results in the lower part of Table 2. The additional Run 1b data will significantly improve the precision of the ratio of branching ratio results.

6. Rare Decays

Rare B decays provide a way to test the standard model against possible effects due an anomalous magnetic moment of the W^\pm , a charged Higgs, etc. Such effects can contribute to the rate of $B \rightarrow \mu^+\mu^-K^{(*)}$ decays. A nice way to measure the rate of $B \rightarrow \mu^+\mu^-K^{(*)}$ decays is to reference it to the observed $B \rightarrow J/\psi K^{(*)}$ signals and use theoretical input to give the expected relative rates and to extrapolate from a limited $\mu^+\mu^-$ mass region to the entire allowed region.¹⁴ CDF has done this in the Run 1a data and obtained the following results (at 90% confidence level):

$$\begin{aligned} BR(B^+ \rightarrow \mu^+\mu^-K^+) &< 3.5 \times 10^{-5} \\ BR(B^0 \rightarrow \mu^+\mu^-K^*(892)^0) &< 5.1 \times 10^{-5} \end{aligned}$$

These results are competitive with the similar limits from UA1 and CLEO.

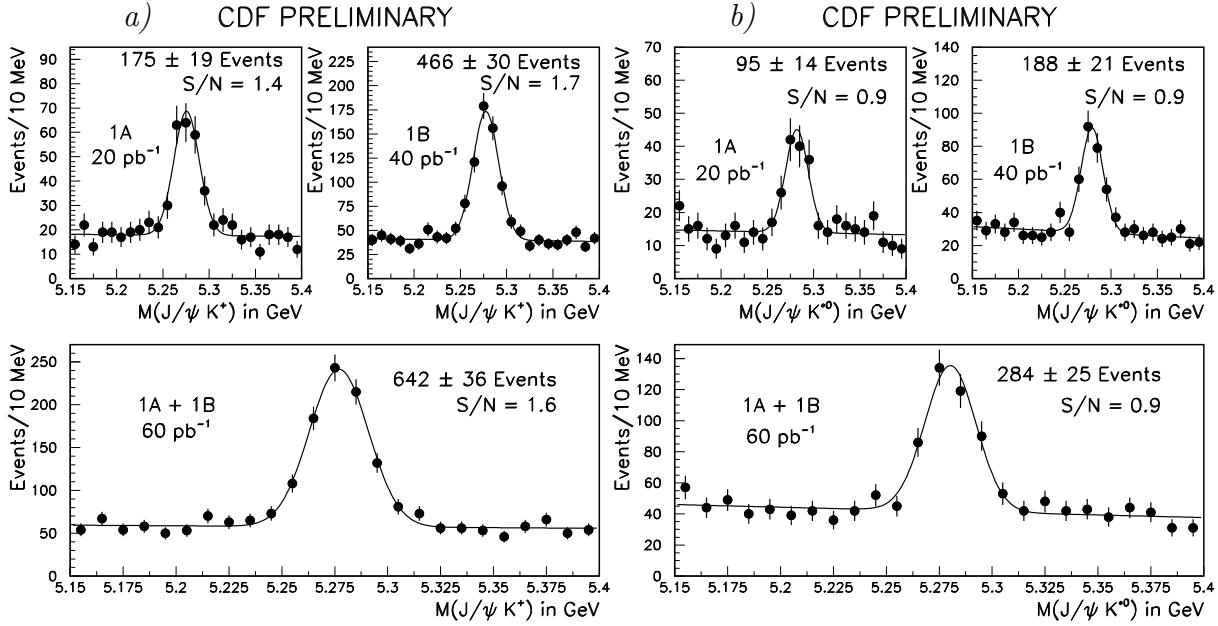


Figure 8: Reconstructed a) $B^+ \rightarrow J/\psi K^+$ and b) $B^0 \rightarrow J/\psi K^*(892)^0$ mass distributions in the 20 pb^{-1} Run 1a, 40 pb^{-1} Run 1b, and combined 60 pb^{-1} Run 1a + 1b data samples.

The decay $B_{d,s}^0 \rightarrow \mu^+ \mu^-$ also tests new particle effects and is forbidden at the tree level. Standard model predictions for the branching ratios are $BR(B_d^0 \rightarrow \mu^+ \mu^-) = 8.0 \times 10^{-11}$ and $BR(B_s^0 \rightarrow \mu^+ \mu^-) = 1.8 \times 10^{-9}$.¹⁵ Some extensions to the standard model predict that $BR(B_s^0 \rightarrow \mu^+ \mu^-)$ can be as large as 10^{-8} .¹⁶ Using dimuon data with invariant mass between 4.9 and $5.8 \text{ GeV}/c^2$ in the Run 1a sample, CDF finds no $B_d^0 \rightarrow \mu^+ \mu^-$ candidates in a mass window of $5.205 - 5.355 \text{ GeV}/c^2$ and 1 $B_s^0 \rightarrow \mu^+ \mu^-$ candidate between $5.300 - 5.450 \text{ GeV}/c^2$. Normalizing to the measured B cross section, $\sigma(B^+) = 2.39 \pm 0.54 \mu\text{b}$ for $p_T(B) > 6 \text{ GeV}/c$ and $|y(B)| < 1$, and assuming $\sigma(B^+) = \sigma(B_d^0) = 3\sigma(B_s^0)$, we find (at 90% confidence level):

$$\begin{aligned} BR(B_d^0 \rightarrow \mu^+ \mu^-) &< 1.6 \times 10^{-6} \\ BR(B_s^0 \rightarrow \mu^+ \mu^-) &< 8.4 \times 10^{-6} \end{aligned}$$

These results are currently the best limits for these decay modes.¹⁷

7. Time-dependent B_d Mixing

The dimuon sample is also used to make the first time-dependent mixing measurement at CDF. Figure 10a illustrates the technique. A vertex-finding algorithm is used to reconstruct a charm vertex in the dimuon sample. The combination of a well-measured charm vertex and one muon can be used to reconstruct the decay length of the parent B hadron, where the charge of the muon gives the flavor of the B hadron at decay. The charge of a second muon from another B hadron indirectly gives the flavor

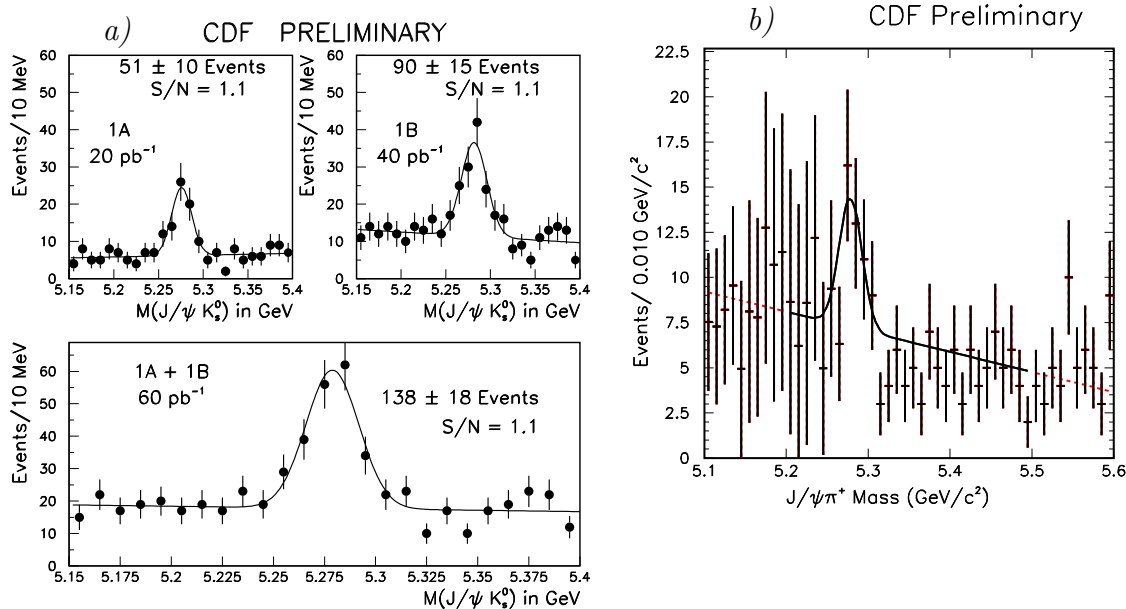


Figure 9: a) Reconstructed $B^0 \rightarrow J/\psi K_S^0$ mass distributions in the 20 pb^{-1} Run 1a, 40 pb^{-1} Run 1b, and combined 60 pb^{-1} Run 1a + 1b data samples. b) Reconstructed $B^+ \rightarrow J/\psi \pi^+$ mass distribution (25.1 ± 8.4 events are observed in $\sim 65 \text{ pb}^{-1}$).

of the first B hadron at production. By measuring the fraction of like sign muon events as a function of the reconstructed pseudo- $c\tau$, the oscillation frequency for $B_d - \bar{B}_d$ mixing, x_d , can be determined.

After requiring the presence of two muons with $p_T(\mu) > 2 \text{ GeV}/c$, a reconstructed charm vertex, and $p_T^{rel}(\mu) > 1.3 \text{ GeV}/c$, the final data sample contains 1516 events with same sign muons and 2357 events with opposite sign muons. The $p_T^{rel}(\mu)$ cut significantly reduces the sequential b decay, $c - \bar{c}$, and fake lepton background contributions.

A binned χ^2 fit to the like sign muon fraction is used to extract x_d , where the mixing from the B_s component of the sample is assumed to be maximal. The B lifetime, the relative fraction of B_d and B_s mesons (from measured LEP values), and the background fraction are constrained in the fit to within their Gaussian errors. Most importantly, the time-dependent contribution of sequential b decays to the like sign muon fraction is also included. Detailed studies have shown that the kinematics of the data sample agree well with the Monte Carlo sample used to model the various background contributions.

Figure 10b shows the like sign muon fraction observed in the data compared with the results for three different cases. In the first case, x_d and x_s are constrained to be zero. Here the expected contribution from sequential B decay and other backgrounds

Table 2. Preliminary CDF Ratio of Branching Ratio Results.

BR Ratio	Measured Value
$\frac{f(b \rightarrow B_d)}{f(b \rightarrow B_u)} \times \frac{BR(B_d \rightarrow J/\psi K^0)}{BR(B_u \rightarrow J/\psi K^+)}$	$1.14 \pm 0.23(\text{stat}) \pm 0.08(\text{syst})$
$\frac{f(b \rightarrow B_d)}{f(b \rightarrow B_u)} \times \frac{BR(B_d \rightarrow J/\psi K^*(892)^0)}{BR(B_u \rightarrow J/\psi K^+)}$	$1.68 \pm 0.34(\text{stat}) \pm 0.22(\text{syst})$
$\frac{f(b \rightarrow B_s)}{f(b \rightarrow B_u)} \times \frac{BR(B_s \rightarrow J/\psi \phi)}{BR(B_u \rightarrow J/\psi K^+)}$	$0.45 \pm 0.11(\text{stat}) \pm 0.07(\text{syst})$
$\frac{f(b \rightarrow B_s)}{f(b \rightarrow B_d)} \times \frac{BR(B_s \rightarrow J/\psi \phi)}{BR(B_d \rightarrow J/\psi K^*(892)^0)}$	$0.27 \pm 0.07(\text{stat}) \pm 0.05(\text{syst})$
$\frac{BR(B_d \rightarrow J/\psi K^0)}{BR(B_u \rightarrow J/\psi K^+)}$	$1.14 \pm 0.23(\text{stat}) \pm 0.08(\text{syst}) \pm ?(b \text{ fraction})$
$\frac{BR(B_d \rightarrow J/\psi K^*(892)^0)}{BR(B_u \rightarrow J/\psi K^+)}$	$1.68 \pm 0.34(\text{stat}) \pm 0.22(\text{syst}) \pm ?(b \text{ fraction})$
$\frac{BR(B_s \rightarrow J/\psi \phi)}{BR(B_u \rightarrow J/\psi K^+)}$	$1.13 \pm 0.28(\text{stat}) \pm 0.18(\text{syst}) \pm ?(b \text{ fraction})$
$\frac{BR(B_s \rightarrow J/\psi \phi)}{BR(B_d \rightarrow J/\psi K^*(892)^0)}$	$0.68 \pm 0.18(\text{stat}) \pm 0.13(\text{syst}) \pm ?(b \text{ fraction})$
$\frac{BR(B_u \rightarrow J/\psi \pi^+)}{BR(B_u \rightarrow J/\psi K^+)}$	$0.049_{-0.017}^{+0.019}(\text{stat}) \pm 0.011(\text{syst})$

is shown. In the second case, x_d is set to zero again and the contribution from maximal B_s mixing is included. The third case gives the final fit results. The CDF preliminary measurement is $x_d = 0.64 \pm 0.18(\text{stat}) \pm 0.21(\text{syst})$. The modeling of the contribution from sequential b decays is the dominant systematic uncertainty and this is expected to be better understood with additional analysis. This measurement has comparable precision to previous results from LEP using a similar technique. Additional measurements of time-dependent mixing can be expected in the future using other data samples.

8. Conclusions

The latest preliminary CDF results on B decays have been presented. The addition of the Run 1b data will continue to improve all the CDF B physics results and allow new measurements so far not possible or expected. This is already seen in the B lifetime results, the observation of the Cabibbo-suppressed $B^+ \rightarrow J/\psi \pi^+$ decay, and in time-dependent mixing measurements. Results on b -baryons, b -tagging, B_s mixing, and other exclusive B decay modes will be coming soon to a conference and journal near you...

References

1. F. Abe et al. (CDF Collaboration), *Nucl. Instrum. Methods Phys. Res., Sect. A* **271**, 387 (1988), and references therein.
2. D. Amidei et al., *Nucl. Instrum. Methods Phys. Res., Sect. A* **350**, 73 (1994); P. Azzi et al., preprint FERMILAB-CONF-94/205-E.
3. V. Chernyak, preprint BudkerINP 95-18; M. Shifman, preprint TPI-MINN-94/32-T.
4. Throughout this paper, references to a specific charge state imply the charge-conjugate state as well.
5. F. Abe et al. (CDF Collaboration), *Phys. Rev. Lett.* **72**, 3456 (1994).
6. L. Montanet et al. (Particle Data Group), *Phys. Rev.* **D50**, 1173 (1994).

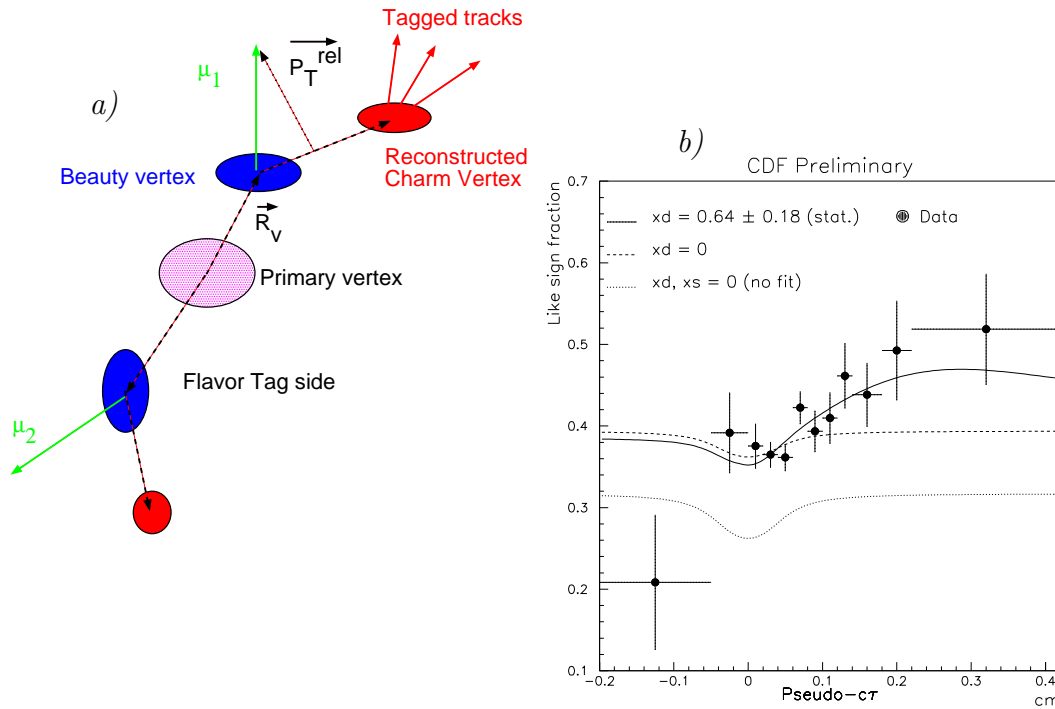


Figure 10: a) Schematic picture of the technique used to measure time-dependent B_d mixing in the CDF dimuon sample. b) Like sign dimuon fraction as a function of pseudo- $c\tau$. The contributions from sequential b decays and background (dotted curve), the addition of maximal B_s mixing (dashed curve), and the observed B_d mixing (solid curve) are shown.

7. See talk by C. Stegmann at this workshop.
8. CLEO Collaboration, *Phys. Rev.* **D43**, 651 (1991).
9. Moriond 95 lifetime averages from the LEP B Lifetimes Working Group.
10. F. Abe et al. (CDF Collaboration), preprint FERMILAB-Pub-94/420-E, accepted by *Phys. Rev. Lett.*
11. I. Dunietz, preprint FERMILAB-PUB-94/361-T; I. Bigi, preprint UND-HEP-94-BIG06.
12. J. Lewis (For the CDF Collaboration), preprint FERMILAB-CONF-94/128-E.
13. CLEO Collaboration, preprint CLNS 94-1291.
14. C. Anway-Wiese (For the CDF Collaboration), preprint FERMILAB-Conf-94/210-E.
15. A. Ali, C. Greub, T. Mannel, Proceedings of the ECFA Workshop on the Physics of the European B Meson Factory (1993), 155.
16. J. L. Hewett et al., *Phys. Rev.* **D39**, 250 (1989).
17. See talk by P. Avery at this workshop.